*Journal of Statistical Physics, Vol. 65, Nos. 3/4, 1991*

# Exact Solution of the Boltzmann Equation in the Homogeneous Color Conductivity Problem

**V. Garzó[1] and A. Santos[1]**

*Received February 15, 1991*

An exact solution of the Boltzmann equation for a binary mixture of "colored" Maxwell molecules is found. The solution corresponds to a nonequilibrium homogeneous steady state created by a nonconservative external force. Explicit expressions for the moments of the distribution function are obtained. By using information theory, an approximate velocity distribution function is constructed, which is exact in the limits of small and large field strengths. Comparison is made between the exact energy flux and the one obtained from the information theory distribution.

**KEY WORDS:** Boltzmann equation; Maxwell molecules; nonlinear transport; information theory.

## 1. INTRODUCTION

Since its formulation in 1872,[1] the nonlinear Boltzmann equation has represented a cornerstone in the kinetic description of dilute simple or multicomponent gases. Closely related equations are also used in the study of other physical problems, such as the dynamics of electrons and phonons in solids or elementary excitations in quantum fluids and plasmas.

Despite the fundamental importance of the Boltzmann equation, the mathematical complexity of its collision term has hindered the discovery of exact solutions. Exact solutions are important as means of gaining insight into nonequilibrium physical mechanisms and also as tests of approximation methods. In the case of spatially homogeneous situations, Bobylev, Krook, and Wu[2] found in 1976 and exact explicit solution for Maxwell

[1] Departamento de Física, Universidad de Extremadura, 06071-Badajoz, Spain.



0022-4715/91/1100-0747$06.50/0 

molecules [particles interacting via a potential $V(r)=\kappa r^{-4}$]. This stimulated important advances.[3] For an inverse power interaction, Nikol'skii[4] has found a transformation that maps any given spatially homogeneous solution onto an inhomogeneous solution. Nevertheless, the solutions obtained in this way correspond to the so-called homoenergetic dilatational flows[5] and do not account for transport phenomena. Physically more interesting are Ikenberry and Truesdell's solution of the Boltzmann equation for planar shear flow at uniform temperature and density[5] and Asmolov *et al.*'s solution for steady energy flow at constant pressure.[6] Both solutions are restricted to Maxwell molecules and are obtained in terms of the moments of the velocity distribution function.

The aim of this paper is to present an exact solution of the Boltzmann equation for a binary mixture. The only previous exact solution for a multicomponent gas we are aware of corresponds to a 2D homogeneous and isotropic system of so-called "very hard particles."[7] On the other hand, we shall consider here a steady nonequilibrium state where self-diffusion takes place. The system is not driven out of equilibrium by concentration gradients, but by the action of a homogeneous, velocity-dependent external force. This way of producing macroscopic flows in homogeneous situations by means of external nonconservative forces has been recently used in molecular dynamics simulations. Shear flow,[8] energy flow,[9] and color conductivity[10,11] have been generated with this method.

The organization of this paper is as follows. The homogeneous color conductivity state is described in Section 2. In Section 3, exact expressions for the first few velocity moments are derived. Since the velocity distribution function is not known exactly, information theory is used in Section 4 to gain some insight into its qualitative features. Finally, some concluding remarks are offered in Section 5.

## 2. HOMOGENEOUS COLOR CONDUCTIVITY STATE

In the homogeneous color conductivity problem,[10–12] the system is a binary mixture constituted by particles of species 1 and particles of species 2. Both types of particles are mechanically identical, the only distinction being a label or "color charge" each particle carries with it. A constant external field is applied that accelerates particles of different species in opposite directions. This induces macroscopic fluxes in spite of the absence of concentration gradients. A drag force is also added to compensate for the increase of temperature.

Let us assume that a steady homogeneous state has been reached. Let $f_r(\mathbf{v})$ be the velocity distribution function of particles of species $r$. The total

distribution function is $f(\mathbf{v}) = f_1(\mathbf{v}) + f_2(\mathbf{v})$. In the low-density imit, $f_1$ and $f_2$ satisfy a coupled set of two Boltzmann equations:

$$\frac{\partial}{\partial \mathbf{v}} \cdot \left[ \frac{\mathbf{F}_1(\mathbf{v})}{m} f_1(\mathbf{v}) \right] = J[f_1, f_1] + J[f_1, f_2]$$

$$= J[f_1, f] \tag{1}$$

and a similar equation for $f_2$. In Eq. (1), $\mathbf{F}_r(\mathbf{v})$ is the external force acting on particles of species $r$, and $J$ is the Boltzmann collision operator, which in standard notation reads[13]

$$J[f_r, f_s] = \int d\mathbf{v}_1 \int d\Omega \, |\mathbf{v} - \mathbf{v}_1| \, \sigma(|\mathbf{v} - \mathbf{v}_1|, \theta)[f_r(\mathbf{v}') f_s(\mathbf{v}_1') - f_r(\mathbf{v}) f_s(\mathbf{v}_1)] \tag{2}$$

At the kinetic level, the external force that produces color diffusion is[10–12]

$$\mathbf{F}_r(\mathbf{v}) = -k_B T \boldsymbol{\varepsilon}_r - \alpha \mathbf{v} \tag{3}$$

where $T$ is the temperature, $\boldsymbol{\varepsilon}_r = \varepsilon_r \mathbf{x}$ is a constant vector that mimics a chemical potential gradient, and $\alpha$ is a thermostat parameter identical for all the particles. Conservation of total momentum (taken to be zero) and energy imposes the constraints

$$n_1 \boldsymbol{\varepsilon}_1 + n_2 \boldsymbol{\varepsilon}_2 = 0 \tag{4}$$

$$\alpha = -\frac{m}{3} \frac{\mathbf{j}_1 \cdot \boldsymbol{\varepsilon}_1}{n_2}$$

$$= -\frac{m}{3} \frac{\mathbf{j}_2 \cdot \boldsymbol{\varepsilon}_2}{n_1} \tag{5}$$

where

$$n_r = \int d\mathbf{v} \, f_r(\mathbf{v}) \tag{6}$$

is the number density and

$$\mathbf{j}_r = \int d\mathbf{v} \, \mathbf{v} f_r(\mathbf{v}) \tag{7}$$

is the particle flux (or color current) of species $r$. Taking into account Eqs. (3) and (4), it is easy to obtain the coupled set

$$-\frac{k_B T}{m} \boldsymbol{\varepsilon}_1 \cdot \frac{\partial}{\partial \mathbf{v}} f_1 - \frac{\alpha}{m} \frac{\partial}{\partial \mathbf{v}} \cdot (\mathbf{v} f_1) = J[f_1, f] \tag{8}$$

$$\frac{k_B T}{m} \frac{n_1}{n_2} \boldsymbol{\varepsilon}_1 \cdot \frac{\partial}{\partial \mathbf{v}} \left( f - \frac{n}{n_1} f_1 \right) - \frac{\alpha}{m} \frac{\partial}{\partial \mathbf{v}} \cdot (\mathbf{v} f) = J[f, f] \tag{9}$$

where $n = n_1 + n_2$. Notice that the total distribution $f$ does not obey a closed equation.

## 3. NONLINEAR TRANSPORT

In general, the set of equations (8) and (9) can only be solved by means of the Chapman–Enskog method.[13] In this method, the solution is expressed as a perturbation expansion around the state of local equilibrium. Truncation of the expansion at the level of the first, second, or third order provides the Navier–Stokes, Burnett, or super-Burnett approximation, respectively. The corresponding expressions for the fluxes are generally not reliable far from equilibrium.

However, the set of equations (8) and (9) can be solved by the moment method if one restricts oneself to Maxwell molecules. In that case, a moment of order $k$ of the collision operator only involves moments of order less than or equal to $k$. For instance,[14]

$$\int d\mathbf{v}\, \mathbf{v} J[f_r, f_s] = -\lambda(n_s \mathbf{j}_r - n_r \mathbf{j}_s) \tag{10}$$

$$\int d\mathbf{v}\, m\mathbf{v}\mathbf{v} J[f_r, f_s] = \lambda' \left[ \left( n_s p_r + n_r p_s + \frac{2}{3} m \mathbf{j}_r \cdot \mathbf{j}_s \right) \mathbb{1} - (n_s \mathbf{P}_r + n_r \mathbf{P}_s) + m(\mathbf{j}_s \mathbf{j}_r + \mathbf{j}_r \mathbf{j}_s) \right] - \lambda(n_s \mathbf{P}_r - n_r \mathbf{P}_s) \tag{11}$$

$$\int d\mathbf{v}\, \frac{m}{2} v^2 \mathbf{v} \mathbf{J}[f_r, f_r] = -\frac{4}{3} \lambda' n_r \mathbf{q}_r \tag{12}$$

In these equations,

$$\lambda = 1.19\pi(\kappa/m)^{1/2} \tag{13}$$

$$\lambda' = 0.925\pi(\kappa/m)^{1/2} \tag{14}$$

are constants

$$\mathbf{P}_r = \int d\mathbf{v}\, m\mathbf{v}\mathbf{v} f_r(\mathbf{v}) \tag{15}$$

is the pressure tensor, $p_r = \frac{1}{3} \operatorname{tr} \mathbf{P}_r$ is the hydrostatic pressure, and

$$\mathbf{q}_r = \int d\mathbf{v}\, \frac{m}{2} v^2 \mathbf{v} f_r(\mathbf{v}) \tag{16}$$

is the energy flux. The moment equations obtained from Eqs. (8) and (9) can be solved following a recursive scheme: if all the moments of $f$ and $f_r$

of order less than $k$ are known, Eq. (9) allows one to obtain the moments of $f$ of order $k$; once these moments are known, Eq. (8) gives the moments of $f_r$ of order $k$. As a starting point, the moments of order zero, $n_1$ and $n$, and the moment of first order $\mathbf{j}=\mathbf{j}_1+\mathbf{j}_2=\mathbf{0}$ are assumed to be given. The first nontrivial moment is $\mathbf{j}_1$. Multiplying both sides of Eq. (8) by $\mathbf{v}$ and integrating, one gets

$$\frac{k_B T}{m} n_1 \boldsymbol{\varepsilon}_1 + \frac{\alpha}{m} \mathbf{j}_1 = -\lambda n \mathbf{j}_1 \tag{17}$$

Due to the coupling between $\alpha$ and $\mathbf{j}_1$, Eq. (5), Eq. (17) is a quadratic equation for $\mathbf{j}_1$. Its physical solution is

$$\mathbf{j}_1 = -\sigma_1(\varepsilon_1)\, n_1 \boldsymbol{\varepsilon}_1 \tag{18}$$

where

$$\sigma_1(\varepsilon_1) = \frac{3}{2} \lambda n \frac{n_2}{n_1} \varepsilon_1^{-2} \left[ \left( 1 + \frac{4}{3} \frac{k_B T}{mn^2 \lambda^2} \frac{n_1}{n_2} \varepsilon_1^2 \right)^{1/2} - 1 \right] \tag{19}$$

Nonequilibrium molecular dynamics simulations corresponding to this state[10,11] are used to measure the self-diffusion coefficient $D$ as the zero-field limit of the color conductivity coefficient $\sigma_1(\varepsilon_1)$:

$$D = \lim_{\varepsilon_1 \to 0} \sigma_1(\varepsilon_1) \tag{20}$$

This represents an efficient alternative to molecular dynamics methods based on the Green–Kubo formula. On the other hand, the system may exhibit interesting physical properties beyond the linear response regime.[11] Here, we will study the nonlinear response of the system, as measured by the dependence of the main fluxes on the field strength, in the case of a dilute gas of Maxwell molecules.

It is convenient to define a dimensionless color conductivity $\sigma^* = \sigma_1/D$, where $D = k_B T/mn\lambda$ is the self-diffusion coefficient of Maxwell molecules,[13] and a dimensionless field strength

$$\begin{aligned} \varepsilon^* &= \left( \frac{2}{3} \frac{k_B T}{mn^2 \lambda^2} \frac{n_1}{n_2} \right)^{1/2} \varepsilon_1 \\ &= -\left( \frac{2}{3} \frac{k_B T}{mn^2 \lambda^2} \frac{n_2}{n_1} \right)^{1/2} \varepsilon_2 \end{aligned} \tag{21}$$

In terms of dimensionless quantities, Eq. (19) becomes

$$\sigma^*(\varepsilon^*) = \varepsilon^{*-2} [(1 + 2\varepsilon^{*2})^{1/2} - 1] \tag{22}$$

This is the most important transport coefficient of the problem. It exhibits a highly nonlinear dependence on the nonequilibrium parameter $\varepsilon^*$. Its power series expansion (Chapman–Enskog expansion) is

$$\sigma^*(\varepsilon^*) = \sum_{k=0}^{\infty} (-1)^k \frac{(2k)!}{2^k k!\,(k+1)!} \varepsilon^{*2k} \tag{23}$$

This series is convergent for $\varepsilon^{*2} < 1/2$. Thus, the Chapman–Enskog expansion is adequate only for states near equilibrium. For instance, the super-Burnett approximation, $\sigma^* \approx 1 - \frac{1}{2}\varepsilon^{*2}$, underestimates the exact value of $\sigma^*$ at $\varepsilon^* = 1$ by about 32%.

The function $\sigma^*(\varepsilon^*)$ is plotted in Fig. 1. As the intensity of the external field increases, the conductivity coefficient decreases. This was also observed by Hoover[15] in his exact solution of the two-body Boltzmann equation for hard particles diffusing under the action of the same external field as considered here. Equation (22) shows that $\sigma^* \sim \sqrt{2}\,|\varepsilon^*|^{-1}$ in the large-field limit. Thus, the color current $\mathbf{j}_r$ grows (in absolute value) with $|\varepsilon^*|$ until reaching a saturation value $|\mathbf{j}_r^{\text{sat}}| = (3n_1 n_2 k_B T/m)^{1/2}$. This upper bound to the mean velocity of a given species is imposed by the conservation of total energy.

Now, let us turn our attention to the pressure tensors. Equation (9) yields

$$\frac{1}{2}\frac{p}{n_2}(\boldsymbol{\varepsilon}_1 \mathbf{j}_1 + \mathbf{j}_1 \boldsymbol{\varepsilon}_1) + \frac{\alpha}{m}\mathbf{P} = -\lambda' n(\mathbf{P} - p\mathbb{1}) \tag{24}$$

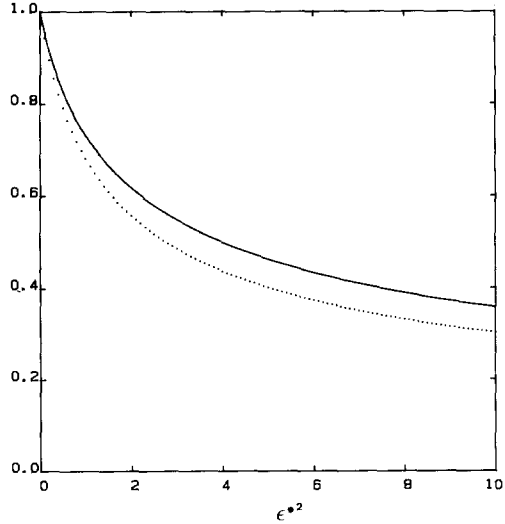


Fig. 1. Plots of the dimensionless color conductivity coefficient $\sigma^*(\varepsilon^*)$ (solid line) and the $yy$ element of the dimensionless pressure tensor $P_{yy}^*(\varepsilon^*)$ (dotted line).

where use has been made of Eq. (11). The dimensionless tensor $\mathbf{P}^* = \mathbf{P}/p$ is diagonal with elements

$$P^*_{yy}(\varepsilon^*) = P^*_{zz}(\varepsilon^*) = \left[1 + \frac{1}{2}\frac{\lambda}{\lambda'}\varepsilon^{*2}\sigma^*(\varepsilon^*)\right]^{-1} \tag{25}$$

$$P^*_{xx}(\varepsilon^*) = 3 - 2P^*_{yy}(\varepsilon^*) \tag{26}$$

The function $P^*_{yy}(\varepsilon^*)$ is also plotted in Fig. 1. We observe that the contribution to the kinetic energy associated with motion orthogonal to the field decreases as the field strength increases. In the large-field limit, $P^*_{yy} \sim (\sqrt{2}\,\lambda'/\lambda)\,|\varepsilon^*|^{-1}$.

The equation for the pressure tensor of species 1 is obtained from Eq. (8):

$$k_B T(\boldsymbol{\varepsilon}_1 \mathbf{j}_1 + \mathbf{j}_1 \boldsymbol{\varepsilon}_1) + 2\frac{\alpha}{m}\mathbf{P}_1 = -\lambda(n\mathbf{P}_1 - n_1\mathbf{P}) + \lambda'[(np_1 + n_1 p)\mathbb{1} - (n\mathbf{P}_1 + n_1\mathbf{P})] \tag{27}$$

Let us introduce the dimensionless pressure tensor $\mathbf{P}^*_1 = \mathbf{P}_1/x_1 p$, where $x_r = n_r/n$ is the molar fraction of species $r$. Thus, we get

$$p^*_1(\varepsilon^*) = \frac{1 + (x_2/x_1)\,\varepsilon^{*2}\sigma^*(\varepsilon^*)}{1 + \varepsilon^{*2}\sigma^*(\varepsilon^*)} \tag{28}$$

$$P^*_{1,yy}(\varepsilon^*) = P^*_{1,zz}(\varepsilon^*) = \frac{1 + p^*_1(\varepsilon^*) + (\lambda/\lambda' - 1)\,P^*_{yy}(\varepsilon^*)}{1 + (\lambda/\lambda')[1 + \varepsilon^{*2}\sigma^*(\varepsilon^*)]} \tag{29}$$

$$P^*_{1,xx}(\varepsilon^*) = 3p^*_1(\varepsilon^*) - 2P^*_{1,yy}(\varepsilon^*) \tag{30}$$

In the large-field limit, $p^*_1 \sim x_2/x_1$ and $P^*_{1,yy} \sim (\lambda'/\lambda\sqrt{2}\,x_1)\,|\varepsilon^*|^{-1}$. Notice that we have $\langle v^2\rangle = \langle \mathbf{v}\rangle^2$ for particles of each species in the limit of $|\varepsilon^*|$ going to infinity. Therefore,

$$\lim_{|\varepsilon^*|\to\infty} f_r(\mathbf{v}) = n_r\delta\left(\mathbf{v} - \frac{\mathbf{j}_r^{\text{sat}}}{n_r}\right) \tag{31}$$

The difference between the pressure tensors $\mathbf{P}^*_1$ and $\mathbf{P}^*$ is of second order in $\varepsilon^*$ and vanishes in the case of an equimolar mixture ($x_1 = x_2$). This suggests to define the tensor

$$\boldsymbol{\Omega}(\varepsilon^*) = \varepsilon^{*-2}\left(\frac{x_2}{x_1} - 1\right)^{-1}[\mathbf{P}^*_1(\varepsilon^*) - \mathbf{P}^*(\varepsilon^*)] \tag{32}$$

which does not depend on the molar fractions. Its elements are

$$\omega(\varepsilon^*) \equiv \frac{1}{3} \operatorname{tr} \boldsymbol{\Omega} = \frac{\sigma^*(\varepsilon^*)}{1+\varepsilon^{*2}\sigma^*(\varepsilon^*)} \tag{33}$$

$$\Omega_{yy}(\varepsilon^*) = \Omega_{zz}(\varepsilon^*) = \frac{\omega(\varepsilon^*)}{1+(\lambda/\lambda')\,\sigma^*(\varepsilon^*)/\omega^*(\varepsilon^*)} \tag{34}$$

The functions $\omega(\varepsilon^*)$ and $\Omega_{yy}(\varepsilon^*)$ are plotted in Fig. 2.

The next moment we are going to evaluate is the energy flux of the whole system $\mathbf{q} = \mathbf{q}_1 + \mathbf{q}_2$. From Eqs. (9) and (12) one gets

$$-\frac{k_B T n_1}{m n_2}\left[\frac{3}{2}\left(p - \frac{n}{n_1} p_1\right)\boldsymbol{\varepsilon}_1 + \boldsymbol{\varepsilon}_1 \cdot \left(\mathbf{P} - \frac{n}{n_1}\mathbf{P}_1\right)\right] + 3\frac{\alpha}{m}\mathbf{q} = -\frac{4}{3}\lambda' n \mathbf{q} \tag{35}$$

whose solution is given by

$$\mathbf{q} = p^2 \frac{1}{m n^2 \lambda'}\left(\frac{x_1}{x_2} - 1\right)\varepsilon^{*2}\gamma(\varepsilon^*)\,\boldsymbol{\varepsilon}_1 \tag{36}$$

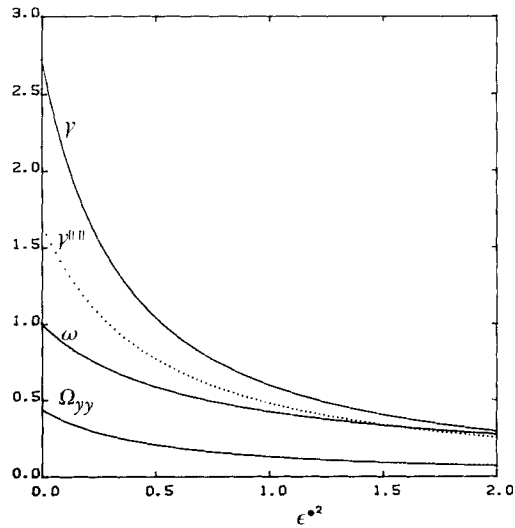


Fig. 2. Plots of the dimensionless functions $\Omega_{yy}(\varepsilon^*)$, $\omega(\varepsilon^*) = \frac{1}{3}\operatorname{tr}\boldsymbol{\Omega}(\varepsilon^*)$, $\gamma(\varepsilon)$, and $\gamma^{(\mathrm{IT})}(\varepsilon^*)$, defined by Eqs. (32), (36), and (48), respectively.

where

$$\gamma(\varepsilon^*) = \frac{3}{4}\frac{(9/2)\,\omega(\varepsilon^*) - 2\Omega_{yy}(\varepsilon^*)}{1 + (9/8)(\lambda/\lambda')\,\varepsilon^{*2}\sigma^*(\varepsilon^*)} \tag{37}$$

In the limit $|\varepsilon^*| \to \infty$, $\gamma \sim (3\lambda'/\sqrt{2}\,\lambda)\,|\varepsilon^*|^{-3}$, which is consistent with Eq. (31). The dimensionless function $\gamma(\varepsilon^*)$ is also plotted in Fig. 2. Notice that the energy flux $\mathbf{q}$ vanishes in the particular case of an equimolar mixture.

## 4. INFORMATION THEORY VELOCITY DISTRIBUTION

Proceeding in a way similar to the one followed in the previous section, we can also obtain higher-order moments. However, we have not been able to obtain an explicit expression for the velocity distribution function. In order to get insight into its qualitative features, we are going to use information theory[16] to construct an approximate velocity distribution function $f_r^{(\mathrm{IT})}(\mathbf{v})$ that maximizes the entropy

$$S_r = -k_B \int d\mathbf{v}\, f_r(\mathbf{v}) \ln\left[\frac{1}{n}\left(\frac{2\pi k_B T}{m}\right)^{3/2} f_r(\mathbf{v})\right] \tag{38}$$

subject to the constraints given by Eqs. (6), (7), and (15). The result is

$$f_r^{(\mathrm{IT})}(\mathbf{v}) = n_r \pi^{-3/2} |\boldsymbol{\Gamma}_r|^{1/2} \exp\left[-\boldsymbol{\Gamma}_r : \left(\mathbf{v} - \frac{\mathbf{j}_r}{n_r}\right)\left(\mathbf{v} - \frac{\mathbf{j}_r}{n_r}\right)\right] \tag{39}$$

where

$$\boldsymbol{\Gamma}_r = \frac{1}{2} m n_r \left(\mathbf{P}_r - \frac{m}{n_r}\mathbf{j}_r\mathbf{j}_r\right)^{-1} \tag{40}$$

Substitution of Eq. (39) into Eq. (38) yields

$$S_1^{(\mathrm{IT})} = \frac{3}{2} n k_B \left\{1 + \frac{1}{3}\ln\left[P_{1,yy}^{*2}\left(P_{1,xx}^* - \frac{3}{2}\frac{x_2}{x_1}\varepsilon^{*2}\sigma^{*2}\right)\right]\right\} \tag{41}$$

This expression represents an upper bound to the entropy corresponding to the actual distribution function. As expected, the nonequilibrium entropy monotonically decreases as we move farther from equilibrium.

The distribution given by Eq. (39) contains all the orders in $\varepsilon^*$ and is exact up to $\varepsilon^{*2}$ (super-Burnett order):

$$f_1(\mathbf{v}) = f_1^{(0)}(\mathbf{v})[1 + \Phi_1^{(1)}(\mathbf{v}^*)\,\varepsilon^* + \Phi_1^{(2)}(\mathbf{v}^*)\,\varepsilon^{*2} + \mathcal{O}(\varepsilon^{*3})] \tag{42}$$

where

$$f_1^{(0)}(\mathbf{v}) = n_1 \left(\frac{m}{2\pi k_B T}\right)^{3/2} e^{-mv^2/2k_B T} \tag{43}$$

$$\Phi_1^{(1)}(\mathbf{v}^*) = -\left(3\frac{x_2}{x_1}\right)^{1/2} v_x^* \tag{44}$$

$$\Phi_1^{(2)}(\mathbf{v}^*) = \left(1-\frac{x_2}{x_1}\right)\left(\frac{3}{2}-v^{*2}\right) + \left[\frac{\lambda}{2\lambda'} - \left(1-\frac{x_2}{x_1}\right)\frac{\lambda}{\lambda+\lambda'}\right](3v_x^{*2}-v^{*2}) \tag{45}$$

$$\mathbf{v}^* \equiv \left(\frac{m}{2k_B T}\right)^{1/2} \mathbf{v} \tag{46}$$

Also, Eq. (39) reduces to the exact form (31) in the limit $|\varepsilon^*| \to \infty$. Thus, one can expect Eq. (39) to give a fair picture of the actual distribution for finite $\varepsilon^*$.

In order to plot the distribution function, it is convenient to introduce the dimensionless quantity

$$\varphi_r^{(\mathrm{IT})}(v_x^*) = \frac{1}{n_1}\left(\frac{m}{2k_B T}\right)^{-1/2} \int_{-\infty}^{+\infty} dv_y \int_{-\infty}^{+\infty} dv_z f_r^{(\mathrm{IT})}(\mathbf{v}) \tag{47}$$

Figures 3 and 4 show $\varphi_1^{(\mathrm{IT})}$, $\varphi_2^{(\mathrm{IT})}$, and $\varphi^{(\mathrm{IT})} = x_1\varphi_1^{(\mathrm{IT})} + x_2\varphi_2^{(\mathrm{IT})}$ for several values of $\varepsilon^*$ and $x_1/x_2$. We can see that for $\varepsilon^*$ large enough, the total function $\varphi^{(\mathrm{IT})}$ exhibits two maxima. Also, $\varphi^{(\mathrm{IT})}$ is symmetric around $v_x^* = 0$ in the equimolar case.

As a quantitative test of the usefulness of the information theory method, let us compare the energy flux obtained from Eq. (39) with the exact one, Eqs. (36) and (37). After some algebra one gets

$$\begin{aligned}\mathbf{q}^{(\mathrm{IT})} &= \int d\mathbf{v}\, \frac{m}{2} v^2 \mathbf{v}[f_1^{(\mathrm{IT})}(\mathbf{v}) + f_2^{(\mathrm{IT})}(\mathbf{v})] \\ &= p^2 \frac{1}{mn^2\lambda'}\left(\frac{x_1}{x_2}-1\right)\varepsilon^{*2}\gamma^{(\mathrm{IT})}(\varepsilon^*)\,\boldsymbol{\varepsilon}_1\end{aligned} \tag{48}$$

where

$$\gamma^{(\mathrm{IT})}(\varepsilon^*) = \frac{\lambda'}{\lambda}\sigma^*(\varepsilon^*)\left[\frac{9}{2}\omega(\varepsilon^*) - 2\,\Omega_{yy}(\varepsilon^*) - \frac{3}{2}\sigma^{*2}(\varepsilon^*)\right] \tag{49}$$

Comparison between $\gamma$ and $\gamma^{(\mathrm{IT})}$ in Fig. 2 shows that $\gamma^{(\mathrm{IT})}$ underestimates the exact value at $\varepsilon^* = 0$ by a factor $(4/3)(3+\lambda/\lambda')/(5+9\lambda/\lambda') = 0.61$. This is a measure of the degree of approximation of Eq. (39) up to third order in $\varepsilon^*$. On the other hand, $\gamma^{(\mathrm{IT})}$ tends to approach $\gamma$ as $|\varepsilon^*|$ increases.

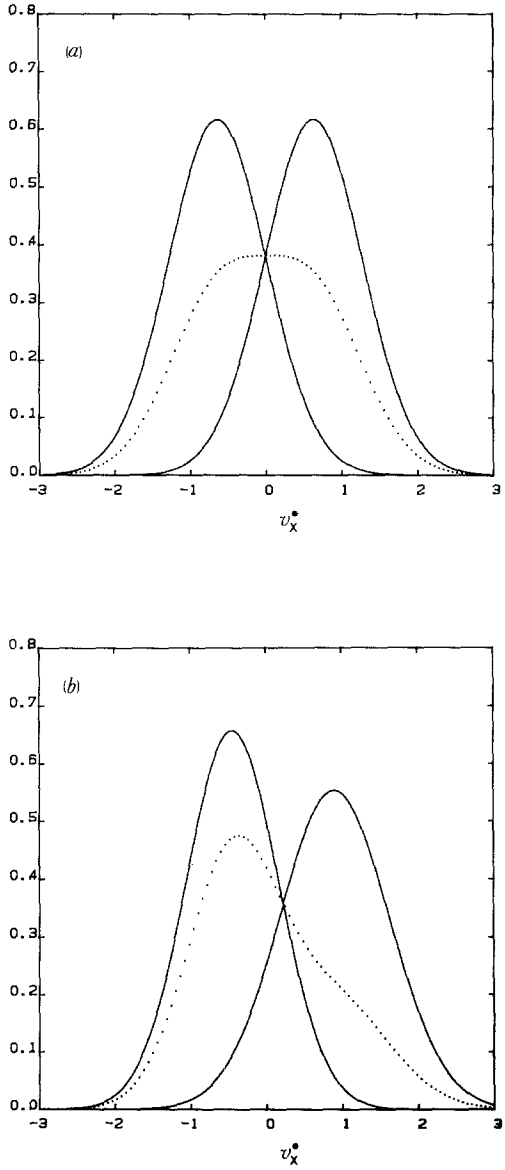


Fig. 3. Plots of the information theory distributions $\varphi_1^{(\mathrm{IT})}(v_x^*)$ (left solid line), $\varphi_2^{(\mathrm{IT})}(v_x^*)$ (right solid line), and $\varphi^{(\mathrm{IT})}(v_x^*)$ (dotted line), defined by Eq. (47), for a value of the field strength $\varepsilon^* = 1$. The values of the molar fractions are (a) $x_1 = x_2 = 1/2$ and (b) $x_1 = 2x_2 = 2/3$.

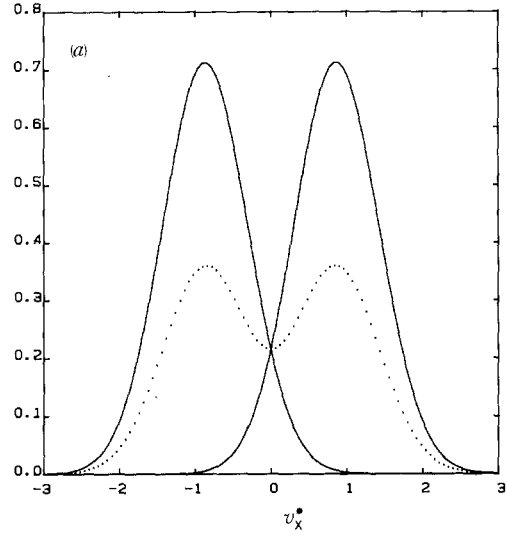


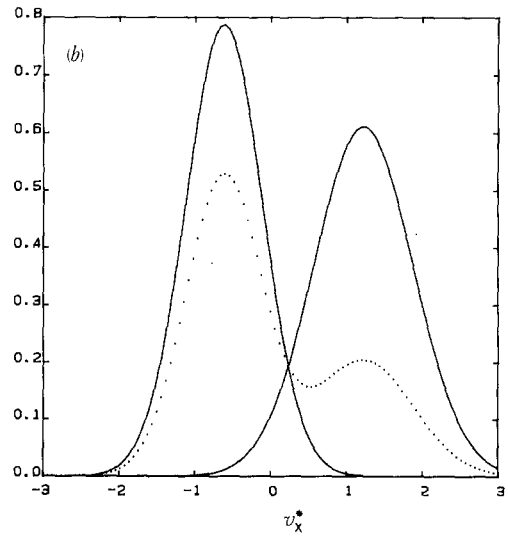


Fig. 4. The same as Fig. 3, but for $\varepsilon^* = 2$.

## 5. CONCLUSIONS

In summary, the hierarchy of moments of the Boltzmann equation for a binary mixture of mechanically identical Maxwell molecules has been exactly solved. It corresponds to a nonequilibrium homogeneous stationary state generated by introducing a homogeneous, velocity-dependent external force. This force accelerates particles of different "colors" along opposite directions, but keeps the temperature constant. The solution shows a highly nonlinear dependence of the fluxes on the field strength. Here, we have obtained the flux of particles, the pressure tensor, and the energy flux vector. Higher-order moments can also be obtained in a recursive way. The Chapman–Enskog expansion of the fluxes is convergent for states close to equilibrium ($\varepsilon^{*2} < 1/2$), but fails otherwise.

In an attempt to construct a velocity distribution function, the information theory method has been used. In the two-body problem,[15] qualitative differences are apparent between the exact and the information theory distributions at moderate fields. However, the approximate distribution obtained here is expected to share the main qualitative aspects with the exact distribution, since it becomes exact up to the super-Burnett order and also in the large-field limit. Comparison between the exact and the approximate energy fluxes shows a good agreement for large field strengths. In order to check the accuracy of the information theory distribution function, one would need to numerically solve the Boltzmann equation. Work is in progress along this line.

We think that the search for exact solutions of the Boltzmann equation, such as the one reported here, is useful in order to improve our understanding of nonequilibrium phenomena outside the linear regime. Moreover, exact solutions play an essential role to test approximation methods, simulation techniques, or model kinetic equations.

## ACKNOWLEDGMENT

Partial support from the Dirección General de Investigación Científica y Técnica (Spain) through grant PS 89-0183 is gratefully acknowledged.

## REFERENCES

1. S. G. Brush, *Kinetic Theory*, Vol. 2 (Pergamon Press, Oxford, 1966).
2. A. V. Bobylev, *Sov. Phys. Doklady* **20**:820, 822 (1976); M. Krook and T. T. Wu, *Phys. Rev. Lett.* **36**:1107 (1976); **38**:991 (1977).
3. M. H. Ernst, *Phys. Rep.* **78**:1 (1981).
4. A. A. Nikol'skii, *Sov. Phys. Doklady* **8**:639 (1964).

5. C. Truesdell and R. G. Muncaster, *Fundamentals of Maxwell's Kinetic Theory of a Simple Monatomic Gas* (Academic Press, New York, 1980).
6. E. S. Asmolov, N. K. Makashev, and V. I. Nosik, *Sov. Phys. Doklady* **24**:892 (1979).
7. E. M. Hendriks and M. H. Ernst, *Physica A* **120**:545 (1983).
8. W. G. Hoover, *Annu. Rev. Phys. Chem.* **34**:103 (1983); D. J. Evans and G. P. Morris, *Comp. Phys. Rep.* **1**:299 (1984).
9. D. J. Evans, *Phys. Lett. A* **91**:457 (1982); M. J. Gillan and M. Dixon, *J. Phys. C* **16**:869 (1983).
10. D. J. Evans, W. G. Hoover, B. Failor, B. Moran, and A. J. C. Ladd, *Phys. Rev. A* **28**:1016 (1983).
11. D. J. Evans, R. M. Lynden-Bell, and G. P. Morris, *Mol. Phys.* **67**:209 (1989).
12. H. A. Posch and W. G. Hoover, *Phys. Rev. A* **38**:473 (1988).
13. S. Chapman and T. G. Cowling, *The Mathematical Theory of Nonuniform Gases* (Cambridge University Press, Cambridge, 1970).
14. L. H. Holway, *Phys. Fluids* **9**:1658 (1966); E. Goldman and L. Sirovich, *Phys. Fluids* **10**:1928 (1967).
15. W. G. Hoover, *J. Stat. Phys.* **42**:587 (1986).
16. C. M. Bender, L. R. Mead, and N. Papanicolau, *J. Math. Phys.* **28**:1016 (1987).